

# Physical, thermal, magnetic and mechanical properties of ARAA

Y.B. Chun <sup>a\*</sup>, D.W. Lee <sup>b</sup>, S. Cho <sup>c</sup>, C.K. Rhee <sup>a</sup>

<sup>a</sup> Nuclear Materials Division, Korea Atomic Energy Research Institute, Daejeon, South Korea

<sup>b</sup> Nuclear Fusion Engineering Development Division, Korea Atomic Energy Research Institute, Daejeon, South Korea

<sup>c</sup> National Fusion Research Institute, Daejeon, Republic of Korea

\*Corresponding author: borobang@gmail.com

## 1. Introduction

Reduced activation ferritic-martensitic (RAFM) steel is considered a primary candidate for the structural material in a fusion reactor, owing to its good swelling resistance and compatibility with various coolants [1]. Several types of RAFM steels showing good performance have been developed [2], which include the European Eurofer 97 [3] and the Japanese F82H [4]. For these alloys, an extensive materials database [5] is available.

The structural materials for the blanket system is expected to be subjected to high heat-load and operate under high-energy (14 MeV) and high-fluence fusion neutron irradiation. The operational range of temperature for a blanket is limited by the high-temperature creep and low-temperature irradiation embrittlement of the structural material. RAFM steels developed thus far are known to be operable at 350-550 °C [6]. To expand the temperature window and thereby allow for various design options, it is important to develop alloys that are able to withstand high temperature and high-energy neutron irradiation.

Since 2011, Korea has put a great deal of efforts to develop the Korean own RAFM steel, from which Zr-containing RAFM steel, ARAA, has been developed. The present work gives a brief introduction on the technological background on the development of ARAA, and presents the physical, thermal, magnetic, and mechanical properties determined from a 5-ton scale ARAA.

## 2. Methods and Results

### 2.1 Experimental Procedures

A 5-ton scale ARAA with a nominal composition of Fe-9Cr-1.2W-0.45Mn-0.2V-0.1C-0.1Si-0.07 Ta-0.01Ti-0.01N-0.01Zr (in wt.%) was produced by a vacuum induction melting (VIM) and then refined by electroslag remelting (ESR). The ingot thus prepared was hot-forged into a slab, following pre-heating at 1200 °C for 3h. The slab was homogenized at 1150 °C for 2h and

then hot-rolled into plates of various thicknesses between 15 mm and 65 mm. All the plates were normalized at 1000°C for 40 min. and then tempered at 750°C for 70 min.

### 2.2 Physical Properties

The density,  $\rho$ , of ARAA at room temperature is 7786 kg/m<sup>3</sup>, which is a slightly higher value than that of Eurofer 97, 7750 kg/m<sup>3</sup> [7]. The density of ARAA exhibits a nearly linear decrease with temperature. A melting point of ARAA, determined from a differential thermal analysis, is 1513 °C. Young's modulus,  $E$ , determined from uni-axial tensile test at room temperature is 208 GPa, and decreased with temperature, being 151 GPa at 600 °C. The Poisson ratio of ARAA determined by measurement of lateral strains during uni-axial tensile loading is 0.3.

The temperatures at which phase transformation takes place were determined by a high resolution dilatometer. The change in length during heating to 1100 °C revealed that transformation from ferrite to austenite starts at ~820 °C ( $A_{Cs}$ ) and finishes at ~885 °C ( $A_{Cf}$ ). Measurement of length of the sample during cooling from the austenite field suggests that martensite transformation starts at ~475 °C ( $T_{Ms}$ ) and is completed at ~280 °C ( $T_{Mf}$ ).

### 2.3 Thermal Properties

The thermal properties of ARAA measured include the coefficient of thermal expansion (CTE), thermal conductivity ( $\kappa$ ), thermal diffusivity ( $\alpha$ ) and specific heat ( $C_p$ ). The CTE of ARAA was measured using a dilatometer. The CTE of ARAA and Eurofer 97 are plotted against temperature in Fig. 1(a). The CTE of ARAA is slightly higher than that of Eurofer 97 and shows a nearly linear increase with temperature. The specific heat of ARAA was determined by a laser flash method, and is plotted against temperature in Fig. 1(b). The  $C_p$  of both ARAA and Eurofer 97 increase roughly linearly with temperature, the slopes of which became steeper at temperatures above 500 °C. The variations of

the thermal conductivity of ARAA and Eurofer 97 with temperature are shown in Fig. 1(c). The  $\kappa$  of both alloys increase with temperature, peaking at 200 °C, and decrease with a further increase of temperature. At temperatures above 450 °C, however, the thermal conductivity of ARAA decreases continuously with temperature, whereas that of Eurofer 97 exhibits an increasing trend again with temperature. The temperature dependency of the thermal conductivity reported for F82H [7] is in accordance with that of ARAA although F82H exhibits slightly higher values in the temperature regime examined.

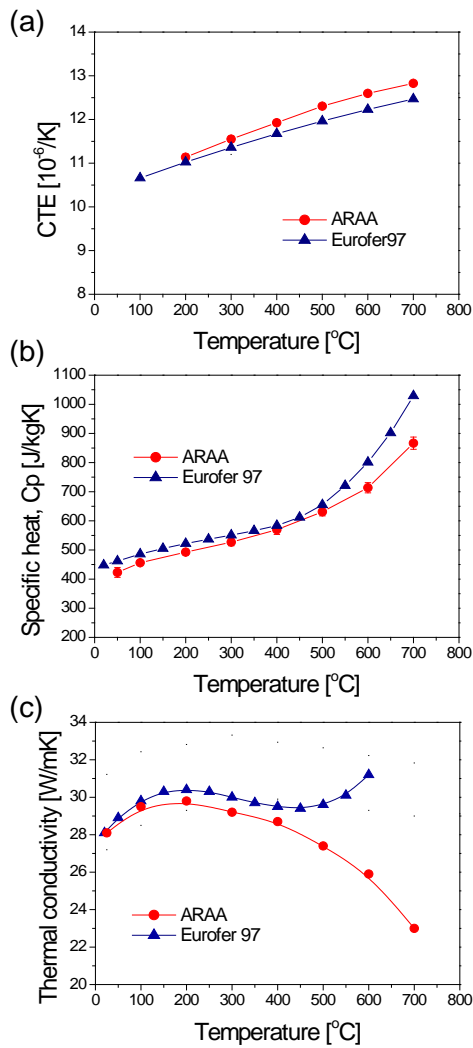


Fig. 1. The variations of thermal properties of ARAA with temperature: (a) the coefficient of thermal expansion, (b) specific heat and (c) thermal conductivity. Standard deviations of data are shown by error bars. The thermal properties of Eurofer 97 [7] are for comparison.

#### 2.4 Magnetic Properties

The Curie temperature,  $T_C$ , was determined by measuring change in power during heating up to 1100 °C, which suggests that the magnetic

transformation of ARAA starts at 720 °C ( $T_{Cs}$ ) and is completed at 760 °C ( $T_{Cf}$ ). The Curie temperature reported for Eurofer 97 is 757 °C [8], which is in accordance with the current result.

Magnetic hysteresis curves (B-H curves) of ARAA were measured in the temperature range between 27 °C and 827 °C using a vibrating sample magnetometer, and the magnetic properties such as the coercive field, remanent magnetization and saturated magnetization were then determined from the curves. The B-H curves determined at various temperatures are shown in Fig. 3. The saturated magnetization decreases with temperature, while the maximum magnetic permeability at a low applied magnetic field is less affected by temperatures up to 727 °C. There was an abrupt decrease of the saturated magnetization at 727 °C, which is due to transition from ferromagnetic to paramagnetic state at just above the Curie temperature.

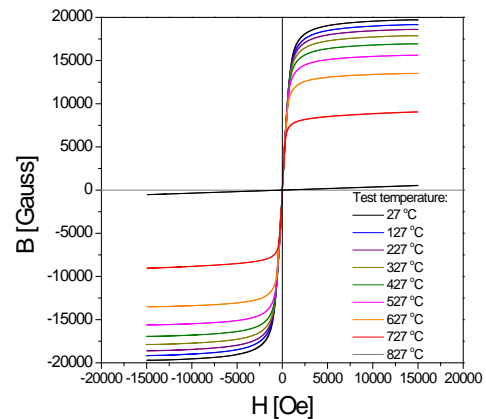


Fig. 2. Magnetic hysteresis curves of ARAA at temperatures between 27 °C and 827 °C.

The coercive field of ARAA at room temperature is 680 A/m and decreases with increasing temperature. A similar trend was reported for Eurofer 97, which, however, shows slightly higher  $H_C$  in the temperature range examined. Such a difference in  $H_C$  between two alloys can be attributed to difference in microstructure, as the coercive field is known to be affected by the distribution characteristics of precipitates and dislocation substructure [9]. From the B-H curves, the remanent magnetization is determined, and it is found that  $M_r$  is 189 Gauss at room temperature, and decreases gradually with temperature, showing a negligible value at 827 °C. Eurofer 97 exhibits a similar temperature dependency but its  $M_r$  values are roughly two times higher than those of ARAA at all temperatures examined [8]. The saturated magnetization of ARAA decreases gradually with increasing temperature up to 627 °C, and is reduced rapidly by a further increase of temperature. At room temperature,

$M_s$  of ARAA is 19,707 Gauss, which is a value slightly higher than that of Eurofer 97 [8].

### 2.5 Mechanical Properties

The tensile properties of ARAA were determined by uni-axial tensile tests at various temperatures up to 600 °C, and the results are shown in Fig. 3. The yield strength of ARAA at room temperature is 522 MPa and decrease with temperature, as shown in Fig. 3(a). The yield strengths of Eurofer 97 at lower temperatures are slightly higher than those of ARAA, and decreases rapidly at temperatures higher than 500 °C. At 600 °C, however, ARAA exhibits slightly higher yield strength than Eurofer 97. The results suggest a reduced temperature dependence of the yield strength of ARAA, which is attribute to solid solution softening effect by the addition of Zr [10].

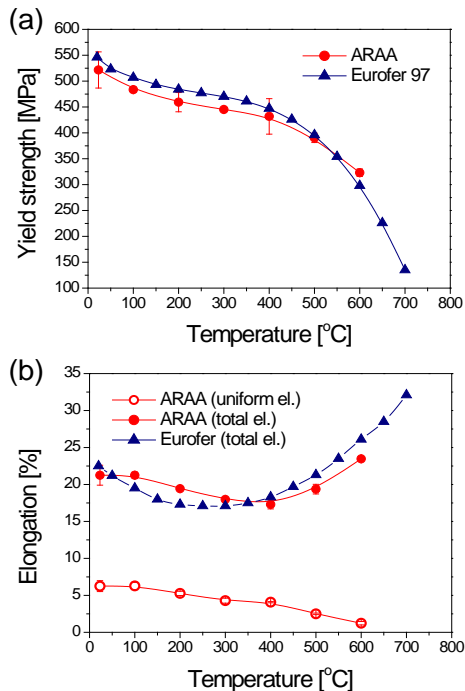


Fig. 3. Temperature dependencies of tensile properties of ARAA: (a) the yield strength and (b) elongation. The data for Eurofer 97 (solid triangle) are given for comparison [7]

The total elongation of ARAA at room temperature is 22% and decreases gradually with temperature, showing the minimum at 400 °C, and then increases with a further increase of temperature, as presented in Fig. 3(b). Eurofer 97 shows a similar trend in temperature dependence of ductility, but shows slightly lower values than ARAA at temperatures up to 400 °C and displays the minimum at 300 °C. The uniform elongation of ARAA, on the other hand, decreases continuously with temperature.

### 3. Conclusions

The mechanical properties of total ninety-eight model alloys designed for application to HCCR TBM in the ITER were evaluated. The addition of small amounts of Zr was found to have positive effects on creep and impact resistance, based on which Zr-containing reduced activation ferritic-martensitic steel, ARAA, has been developed. A 5-ton scale ARAA was produced via VIM and ESR methods and its basic properties required for fusion reactor applications were evaluated. It is found that the physical, thermal, magnetic and mechanical properties of ARAA are comparable to those of Eurofer 97.

### REFERENCES

- [1] R.J. Kurtz, A. Alamo, E. Lucon, Q. Huang, S. Jitsukawa, A. Kimura, R.L. Klueh, G.R. Odette, C. Petersen, M.A. Sokolov, P. Spätig, J.-W. Rensman, Recent progress toward development of reduced activation ferritic/ martensitic steels for fusion structural applications, *Journal of Nuclear Materials* 386-388 (2009) 411-417.
- [2] R.L. Klueh, D.R. Harries, High-Chromium Ferritic and Martensitic Steels for Nuclear Applications, ASTM Stock Number: MONO03, 2001
- [3] B. van der Schaaf, F. Tavassoli, C. Fazio, E. Rigal, E. Diegele, R. Lindau, G. LeMarois, The development of EUROFER reduced activation steel, *Fusion Engineering and Design* 69 (2003) 197-203.
- [4] Y. Kohno, D.S. Gelles, A. Kohyama, M. Tamura, A. Hishinuma, Irradiation response of a reduced activation Fe-8Cr-2W martensitic steel (F82H) after FFTF irradiation, *Journal of Nuclear Materials* 191-194 (1992) 868-873.
- [5] H. Tanigawa, K. Shiba, A. Möslang, R.E. Stoller, R. Lindau, M.A. Sokolov, G.R. Odette, R.J. Kurtz, S. Jitsukawa, Status and key issues of reduced activation ferritic/martensitic steels as the structural material for a DEMO blanket, *Journal of Nuclear Materials* 417 (2011) 9-15.
- [6] N. Baluc, D.S. Gelles, S. Jitsukawa, A. Kimura, R.L. Klueh, G.R. Odette, B. van der Schaaf, J. Yu, Status of reduced activation ferritic/martensitic steel development, *J. Nucl. Mater.*, 367-370 (2007) 33-41.
- [7] F. Tavassoli, Fusion Demo Interim Structural Design Criteria (DISDC), Appendix A Material Design Limit Data, A3. S18E Eurofer Steel, 2004.
- [8] K. Mergia, N. Boukos, Structural, thermal, electrical and magnetic properties of Eurofer 97 steel, *Journal of Nuclear Materials* 373 (2008) 1-8.
- [9] L.J. Dykstra, in: A.E. Berkowitz, E. Kneller (Eds.), *Magnetism and Metallurgy*, Academic Press, 1969.
- [10] Y.B. Chun, D.W. Lee, S. Cho, C.K. Rhee, Improvement of creep and impact resistance of reduced activation ferritic-martensitic steel by the addition of Zr, *Materials Science and Engineering A*, in press, DOI: 10.1016/j.msea.2015.08.033
- [11] J. Aktaa, M. Weick, M. Walter, High Temperature Creep-Fatigue Structural Design Criteria for Fusion Components Built from EUROFER 97, FZKA 7309, 2007.